International Journal of Computer Science and Information Technology
ISSN: 3005-9682 (Print), ISSN: 3005-7140 (Online) | Volume 3, Number 3, Year 2024
DOI: https://doi.org/10.62051/ijcsit.v3n3.07
Journal homepage: https://wepub.org/index.php/IJCSIT/index

Comparison of Pansharpening Methods Based on Fengyun-4B GHI

Zhe Peng

School of Surveying and Land Information Engineering, Henan Polytechnic University, Jiaozuo 454003, China

ABSTRACT

Pansharpening aims to improve the spatial resolution of multispectral (MS) images while maintaining their spectral properties, which is very important for military reconnaissance, environmental monitoring, urban planning, and other fields that require high-resolution remote sensing data. With the continuous development of global satellite technology, various new types of sensors have emerged, and the data obtained from different sensors provide valuable resources for scientific research. The fast imager GHI on board the Fengyun-4B star (FY-4B) provides 250m panchromatic (PAN) images and 500m MS images. In order to obtain the desired images at the highest spatial resolution, fusion of the original MS images with the high spatial resolution PAN images using pansharpening techniques to generate high-resolution multispectral images is a feasible way. In this paper, nine commonly used pansharpening algorithms are used to perform synthetic and real experiments on GHI data, and the SFIM method demonstrates excellent performance in both visual and various quantitative metrics evaluations, which are able to accurately retain the spectral properties of the original images while improving the spatial resolution of the images.

KEYWORDS

Pansharpening; Fast imager (GHI); PAN image; MS image

1. INTRODUCTION

The fast imager on board FY-4B is the world's first day-night high-frequency imaging instrument, capable of providing continuous observation of a 2000 km × 2000 km area at 1-minute intervals across multiple spectral bands. This flexibility and precision enhance the monitoring of typhoons, heavy rainfall, and mesoscale hazardous weather events. Satellite sensors like GHI, due to their unique advantages in design, can capture multiple spectral bands with different spatial resolutions. The main advantage of these sensors lies in their ability to record all spectral bands nearly simultaneously, effectively avoiding issues caused by temporal variations and ensuring consistent lighting and atmospheric conditions. Furthermore, the observation directions of all bands remain nearly the same, resulting in very high co-registration accuracy between the bands. However, due to various physical and technical limitations of different sensors, achieving both high spatial and spectral resolution images with a single sensor is not feasible [1]. This is primarily due to three reasons: first, limitations in storage and transmission bandwidth; second, improving the signal-to-noise ratio of certain bands through increased pixel size; and third, some bands are designed for specific purposes and do not require high spatial resolution, such as those used for atmospheric correction. Nevertheless, there is still a desire to obtain all bands at the highest spatial resolution, which raises the question: is it possible to use pansharpening techniques to enhance the spatial resolution of remote sensing images while preserving the spectral information of the original remote sensing images, thereby supporting more detailed and accurate information extraction? Pansharpening technology plays a crucial role in

Content from this work may be used under the terms of CC BY-NC 4.0 licence (https://creativecommons.org/licenses/by-nc/4.0/). Published by Warwick Evans Publishing.

key areas such as environmental monitoring, land resource utilization, precision agriculture, urban planning, and military reconnaissance [2].

Currently, many pansharpening algorithms have been developed. Some methods excel in preserving spatial resolution, while others prioritize spectral resolution, giving them a comparative advantage. However, there is always a trade-off between the two. Currently, common pansharpening methods can be classified into two types: component substitution (CS)-based methods and multi-resolution analysis (MRA)-based methods.

2. PANSHARPENING METHODS

2.1. Pansharpening Theory

Pansharpening methods combine the spectral information of low-resolution MS images with the geometric information of high-resolution panchromatic images, resulting in a high-resolution MS image [3]. Pansharpening is the fusion of different images, characterized by a better description of certain objects under different conditions. Therefore, it is not necessary to individually consider the limitations of each image. This is an important task in the field of remote sensing data fusion, which combines three or more low-resolution MS images with a high-resolution panchromatic image to provide more accurate and higher-quality color images [4]. Pansharpening technology is a vital step in satellite image processing, as the fused images not only retain the advantageous information in terms of spectral, spatial, and temporal resolutions but also address the deficiencies of single sensor images in these aspects.

2.2. CS-based Methods

CS-based methods are the simplest and most widely used techniques in the series of pansharpening methods. The core idea is to transform the MS image into a new space based on spectral variations and then use the PAN image to replace the spatial components, followed by applying an inverse transformation to obtain the pansharpened image. Typical CS-based methods include brovey transformation (Brovey)[5], intensity-hue-saturation (IHS) [6], principal component analysis (PCA) [7], Gram-Schmidt (GS) [8], Gram-Schmidt adaptive (GSA) [9], and partial replacement adaptive component substitution (PRACS) [10]. These methods approximate the PAN image through linear combinations of MS bands, and the pansharpening performance largely depends on the definition of the weights. Therefore, these methods can effectively retain the high spatial quality of the fused image but are prone to spectral distortions, especially when the correlation between the PAN image and the MS image is low, often resulting in unstable performance of CS-based methods.

2.3. MRA-based Methods

MRA methods address the pansharpening problem from a spatial perspective, injecting spatial details generated from the multi-resolution decomposition of the PAN image. These methods utilize techniques such as curve transforms, Laplacian pyramids, or wavelet transforms to decompose both the MS image and the PAN image into multiple scales. They then extract the spatial information from the PAN image at a specific scale and inject it into the corresponding scale of the MS image decomposition, ultimately generating the fused image through an inverse transformation of the decomposition process. Typical MRA-based methods include high-pass filter (HPF) [11], Wavelet Transform (Wavelet) [12], smoothing filter based on intensity modulation (SFIM) [13], the GLP based on Gaussian filters matches the MTF of an MS sensor (MTF-GLP) [14], and MTF-GLP with HPM (MTF-GLP-HPM) [15]. Usually MRA methods maintain the structural integrity of the original PAN image during the downscaling process, they often provide better spectral fidelity performance compared to CS-based methods. However, due to aliasing effects, they may cause severe spatial distortion.

2.4. Quality Metrics Based on Reference Images

2.4.1. Peak Signal-to-Noise Ratio (PSNR)

Peak Signal-to-Noise Ratio is a widely used measurement method for assessing image spatial quality. It is calculated by dividing the number of gray levels in the image by the same pixel values in the reference image and the fused image. A higher PSNR value indicates less image distortion, indicating a better fusion effect. The calculation formula is as follows:

$$\mathrm{PSNR} = 20\lg\left\{\frac{L}{\frac{1}{MN}\sum_{i=1}^{M}\sum_{j=1}^{N}\left(F_{(i,j)} - P_{(i,j)}\right)^2}\right\} \tag{1}$$

In the formula, L represents the number of gray levels; M and N are the length and width of the image, respectively; and $F_{(i,j)}$ and $P_{(i,j)}$ represent the gray values at coordinates (i,j) for the reference image and the pansharpened image, respectively.

2.4.2. Structural Similarity (SSIM)

The structural similarity index is used to determine the structural similarity between the fused image and the reference image. The greater the value of the structural similarity index, the better the structural similarity, indicating a better fusion effect. The calculation formula is:

$$\mathrm{SSIM} = \frac{\left(2m_X m_Y + C_1\right) 2s_{XY} + C_2}{\left(s_X^2 + s_Y^2 + C_2\right) m_X^2 + m_Y^2 + C_1} \tag{2}$$

In this formula, m_X and m_Y are the means of the reference and fused images, respectively; s_{XY} represents the covariance of the reference and fused images; s_X and s_Y are the standard deviations of the reference and fused images, respectively. The values of the structural similarity index range from -1 to +1; the closer the value is to +1, the more similar the fused image is to the reference image, indicating a better fusion effect.

2.4.3. Spectral Angle Mapper (SAM)

The spectral angle mapper is used to measure the degree of spectral distortion between the fused image and the reference image. It is defined as the angle between the spectral vector of the fused image and the spectral vector of the reference image at the same pixel. The smaller the spectral angle, the less distortion there is between the fused image and the reference image, indicating a better fusion effect. Conversely, a larger spectral angle indicates greater distortion between the fused image and reference image, leading to a poorer fusion effect. The calculation formula is:

$$\mathrm{SAM}\left(X_1, X_2\right) = \arccos\left(\frac{X_1 \cdot X_2}{|X_1| \cdot |X_2|}\right) \tag{3}$$

Here, X_1 and X_2 represent two spectral vectors. The average SAM value across all images provides a global measure of spectral distortion, with an ideal value of 0 for a perfectly fused image.

2.4.4. Relative Global Error (ERGAS)

Relative Global Error is a commonly used global quality index that assesses the quality of the fused image. A smaller ERGAS value indicates greater similarity between the fused image and the reference image, reflecting better spectral fidelity and fusion effect. The calculation formula is:

$$\mathrm{ERGAS} = 100\frac{h}{l}\sqrt{\frac{1}{N}\sum_{i=1}^{N}\left(\frac{\mathrm{RMSE}(B_i)}{M(B_i)}\right)^2} \tag{4}$$

In this formula, h and l represent the spatial resolutions of the panchromatic and multispectral images, respectively; $\mathrm{RMSE}(B_i)$ is the root mean square error between the fused image and the reference image for the i th band; $M(B_i)$ represents the average radiance of the original MS band; and N is the number of fused bands.

2.4.5. Correlation Coefficient (CC)

The correlation coefficient is a widely used metric for measuring the quality of image fusion, reflecting the similarity of spectral characteristics between the fused image and the reference image. When the absolute value of CC is close to 1, it indicates better spectral fidelity of the fused image, resulting in a superior fusion effect. It is defined as:

$$\mathrm{CC} = \frac{\sum_{i=1}^{w}\sum_{j=1}^{h}\left(\left(X_{i,j}-\mu_X\right)\left(Y_{i,j}-\mu_Y\right)\right)}{\sqrt{\sum_{i=1}^{w}\sum_{j=1}^{h}\left(X_{i,j}-\mu_X\right)^2\sum_{i=1}^{w}\sum_{j=1}^{h}\left(Y_{i,j}-\mu_Y\right)^2}} \tag{5}$$

In this expression, w and h indicate the width and height of the image, respectively; m_X and m_Y represent the means of the reference image and the pansharpened image, respectively. The range of CC is from -1 to +1, with an ideal value being +1.

2.4.6. Root Mean Square Error (RMSE)

Root Mean Square Error evaluates the differences between the fused image FF and the reference image PP by calculating the variation of pixel values. The smaller the RMSE value, the better the fusion effect. The calculation formula is:

$$\mathrm{RMSE} = \sqrt{\frac{1}{M_1 N_1}\sum_{i=1}^{M_1}\sum_{j=1}^{N_1}\left(F_{(i,j)}-P_{(i,j)}\right)^2} \tag{6}$$

In this formula, M and N are the length and width of the images, respectively; $F_{(i,j)}$ and $P_{(i,j)}$ are the gray values at coordinate (i, j) for the reference image and the pansharpened image, respectively.

2.5. No-Reference Image Quality Metrics (QNR)

No-reference image quality metrics (QNR) are used to evaluate the pansharpened image based on the levels of spatial and spectral distortion in the absence of a reference image. The calculation formula is:

$$QNR = \left(1-D_l\right)^a\left(1-D_s\right)^b \tag{7}$$

Where a and b are weighting coefficients. D_l and D_s are distortion indices for spectral and spatial aspects, respectively. Smaller indices D_l and D_s indicate that the pansharpened full-resolution MS image has less spectral and spatial distortion. QNR is a composite index, and a higher QNR value indicates better quality of the pansharpened full-resolution MS image.

3. EXPERIMENT AND ANALYSIS

In this section, we conducted experiments using nine Pansharpening methods: Brovey, IHS, PCA, GS, GSA, Wavele, MTF_GLP, MTF_GLP_HPM, and SFIM, on a GHI image collected on January 30, 2023. The GHI image is located in the North China Plain and Bohai Sea area, consisting of a 250m PAN image and the first three bands of the 500m MS image. To thoroughly evaluate the performance of the nine methods, we designed both synthetic (low-resolution) experiments and real (full-resolution) experiments.

3.1. Synthetic Experiment

In the synthetic experiments, to ensure the presence of a true reference image, the GHI data comprised a 250m PAN image and the first three bands (B1, B2, B3) of the 500m MS image, which were upsampled by a factor of 2 using a point spread function (PSF), resulting in a 500m PAN image and a 1000m MS image. By using different downscaling methods on the 500m PAN image and the 1000m MS image after Pansharpening, we produced a 500m Pansharpened MS image that could be objectively evaluated against the original 500m MS image, effectively using the original 500m MS image as the reference.

Figure 1 shows the Pansharpened true-color results (displayed in a B3, B2, B1 band combination) of the GHI data after downscaling the enlarged MS image from 1000m to 500m using various Pansharpening methods. From the Pansharpened results, it is evident that all methods effectively improve spatial resolution, but the CS-based methods (Brovey, IHS, PCA, GS) exhibit significant spectral distortion. The Pansharpened results of Brovey, IHS, and GS show darker colors in land and cloudy areas compared to the reference MS image, while the colors appear brighter in the sea areas. In contrast, the PCA method shows brighter colors in land and cloudy areas when compared to the reference MS image, which is the opposite of the first three methods. The GSA method, among the CS-based methods, is the closest to the reference MS image in color and shows less spectral distortion.

Compared to the CS-based methods, the four MRA-based methods (Wavele, MTF_GLP, MTF_GLP_HPM, and SFIM) maintain the spectral characteristics of the MS images well, exhibiting less spectral distortion. Figure 2 presents the absolute difference residual images obtained by subtracting the Pansharpened MS images from the reference MS image shown in Figure 1, with the mean residual DN value calculated for each method in the title section. From Figure 2, it is evident that the four methods (Brovey, IHS, PCA, GS) have more high-value regions in the sea and cloudy areas, indicating greater spatial information loss and spectral distortion. The GSA method shows some high-value regions over the sea, indicating less spatial information loss and spectral distortion. Wavele, MTF_GLP, and MTF_GLP_HPM follow, with SFIM demonstrating the least spectral distortion. Furthermore, the SFIM method has the smallest mean residual DN value of 6.2243, indicating relatively lower spectral distortion and spatial detail loss compared to the other methods.

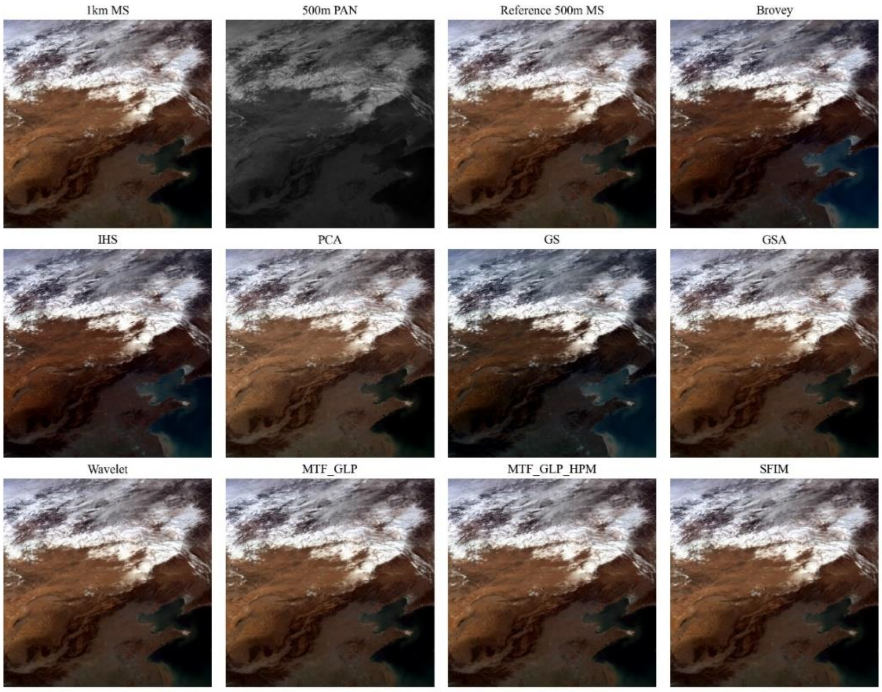

Figure 1. Pansharpened MS results of each method in the synthetic experiment compared with the 1000m MS image and the 500m PAN image.

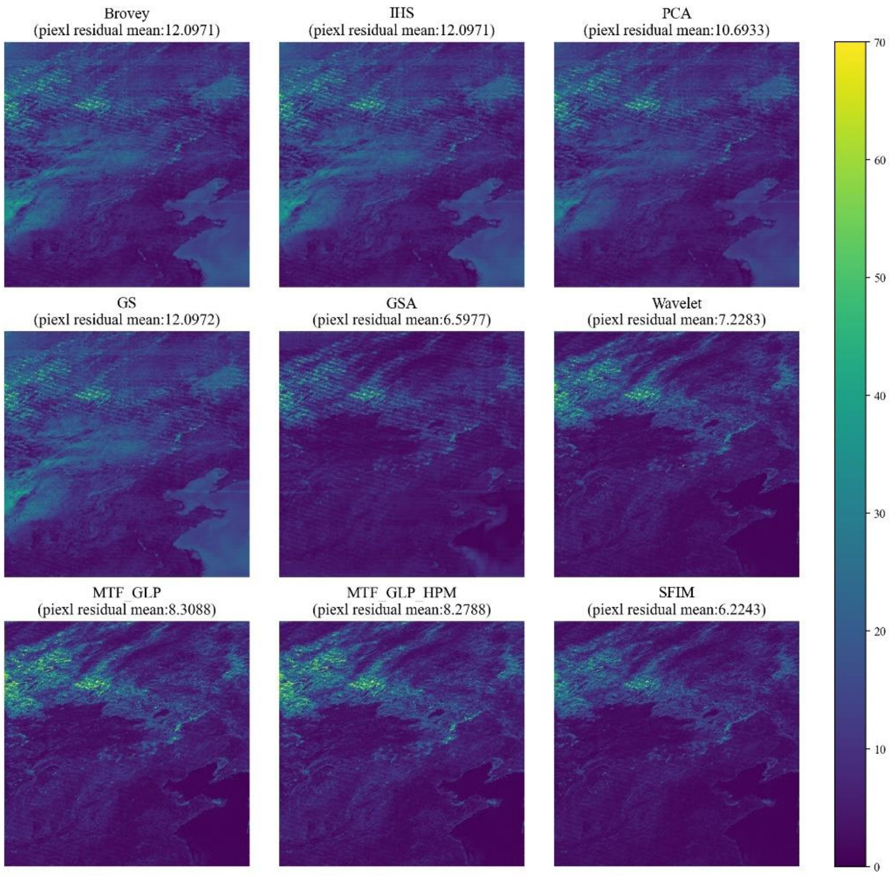

Figure 2. Residual images of the nine pansharpening results from GHI data compared with the original MS image in the synthetic experiment.

Distinguishing the subtle differences between the Pansharpening results of the nine competing methods through visual inspection alone is challenging, especially when two methods perform similarly. In Table I, we employed six reference-based quality metrics to validate the Pansharpened MS images, marking the ideal values for each method in the second row. PSNR can verify the quality of spatial information in the fused image, reflecting whether noise has been suppressed in the Pansharpened image; a higher PSNR value indicates more information is retained post-fusion, representing better fusion quality. SSIM, SAM, CC, and RMSE are metrics that reflect the spectral information of the Pansharpened result images. ERGAS evaluates the global information of the Pansharpened result images. The results shown in Table I indicate that the quantitative evaluation is consistent with the visual comparison: the CS-based methods generally performed worse across all metrics compared to the MRA-based methods, although the GSA method performed remarkably well among the CS methods. Meanwhile, the SFIM method outperformed all others across the six metrics. This indicates that the Pansharpening results from the SFIM method have superior capabilities in retaining spatial and spectral information compared to the other methods when applied to the GHI data.

Table 1. Quantitative assessment of pansharpening results for GHI data in the synthetic experiment.

	PSNR	SSIM	SAM	ERGAS	CC	RMSE
Ideal	$+\infty$	1	0	0	1	0
PCA	42.7127	0.9940	0.0472	2.4577	0.9975	29.9655
Brovey	48.0362	0.9949	0.0045	1.3350	0.9969	16.2346
IHS	48.1029	0.9949	0.0051	1.3300	0.9969	16.1104
GS	48.1065	0.9950	0.0052	1.3299	0.9970	16.1038
MTF_GLP	48.5244	0.9926	0.0039	1.2627	0.9973	15.3473
MTF_GLP_HPM	48.6768	0.9927	0.0040	1.2415	0.9974	15.0805
Wavelet	49.4164	0.9929	0.0062	1.1417	0.9977	13.8496
GSA	50.8619	0.9954	0.0044	0.9713	0.9984	11.7262
SFIM	51.1812	0.9957	0.0043	0.9331	0.9985	11.3030

Bold values indicate the most accurate result in each case.

3.2. Real Experiment

In the real experiment, the 250m PAN image from the GHI data was used to pansharpen the 500m MS image down to 250m, generating full-resolution MS images using various pansharpening methods. Following this strategy, there was no 250m reference MS image available to validate the pansharpening results of the GHI data. Therefore, we have listed the values of the nine methods on the no-reference image quality assessment metric QNR in Table II.Based on the results in Table II, the real experiment yielded results similar to the synthetic experiment: the pansharpening results based on MRA methods generally performed better than those based on CS methods. However, the GSA and Wavelet methods did not perform well in the real experiment, while the SFIM method exhibited the highest QNR value, indicating that SFIM still has superior capabilities in retaining spatial and spectral information compared to other methods in the real experiment.Figure 3 shows the results of the full-resolution MS image pansharpened to 250m using the SFIM method in comparison with the 500m MS image and the 250m PAN image. It is clear that the full-resolution MS image obtained using the SFIM method appears visually clearer, and its spectral properties have been accurately preserved.

Table 2. Quantitative assessment of pansharpening results for GHI data in the real experiment.

	Brovey	IHS	GS	PCA	Wavelet	GSA	MTF_GLP	MTF_GLP_HPM	SFIM
QNR	0.9152	0.9161	0.9241	0.9245	0.9483	0.9502	0.9724	0.9729	0.9815

Bold values indicate the most accurate result in each case.

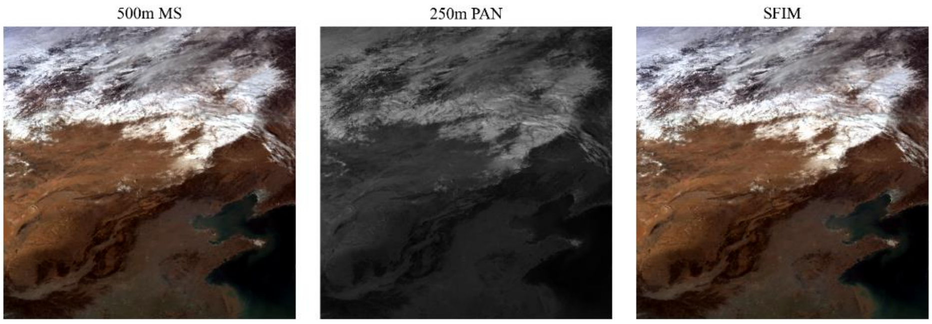

Figure 3. Comparison of the full-resolution MS results after pansharpening using the SFIM method with the 500m MS image and the 250m PAN image in the real experiment.

4. CONCLUSION

This study comprehensively evaluated the performance of nine pansharpening algorithms for GHI data from the FY-4B satellite's rapid imaging sensor. Through synthetic and real experiments on GHI images, we explored the capabilities of different algorithms in enhancing spatial resolution and preserving spectral properties. The experimental results demonstrated that methods based on MRA generally outperform those based on CS, with SFIM algorithm showing the best performance. The SFIM algorithm exhibited exceptional performance in both visual and quantitative assessments; it not only effectively enhanced the spatial resolution of images but also maintained spectral properties well. Additionally, it achieved the highest value in the no-reference image quality metric QNR, further confirming its superiority in real experiments. Overall, the SFIM algorithm provides high-quality pansharpening results for FY-4B GHI imagery, meeting the application demands of high-resolution remote sensing data in fields such as weather analysis and forecasting, as well as environmental and disaster monitoring.

REFERENCES

[1] Ye F, Guo Y, Zhuang P. Pan-sharpening via a gradient-based deep network prior [J]. Signal Processing Image Communication, 2019, 74:322-331.DOI:10.1016/j.image.2019.03.004.

[2] WANG P, YAO H, LI C, et al. Multiresolution Analysis Based on Dual-Scale Regression for Pansharpening [J]. IEEE Transactions on Geoscience and Remote Sensing, 2022, 60: 1-19.

[3] Vivone G, Alparone L, Chanussot J, et al. A Critical Comparison Among Pansharpening Algorithms [J]. IEEE Transactions on Geoence & Remote Sensing, 2015, 53(5):2565-2586.DOI:10.1109/TGRS.2014.2361734.

[4] Xiangchao M, Huanfeng S, Huifang L, et al. Review of the Pansharpening Methods for Remote Sensing Images Based on the Idea of Meta-analysis: Practical Discussion and Challenges [J]. Information Fusion, 2018, 46:S1566253517306036-. DOI:10.1016/j.inffus.2018.05.006.

[5] Gillespie A R, Kahle A B, Walker R E. Color enhancement of highly correlated images. II. Channel ratio and "chromaticity" transformation techniques – ScienceDirect [J]. Remote Sensing of Environment, 1987, 22(3):343-365. DOI:10.1016/0034-4257(87)90088-5.

[6] CARPER W J, LILLESAND T M, KIEFER P W J P E, SENSING R. The use of intensity-hue-saturation transformations for merging SPOT panchromatic and multispectral image data [J]. Photogrammetric Engineering and Remote Sensing, 1990, 56(4).

[7] CHAVEZ J P, KWARTENG A. Extracting spectral contrast in Landsat Thematic Mapper image data using selective principal component analysis [J]. Photogrammetric Engineering and Remote Sensing, 1989, 55: 339-48.

[8] LABEN C A, BROWER B V. Process for enhancing the spatial resolution of multispectral imagery using pan-sharpening [Z]. Google Patents. 2000: U.S. Patent 6011875

[9] AIAZZI B, BARONTI S, SELVA M. Improving Component Substitution Pansharpening Through Multivariate Regression of MS+Pan Data [J]. IEEE Transactions on Geoscience and Remote Sensing, 2007, 45(10): 3230-9.

[10] CHOI J, YU K, KIM Y. A New Adaptive Component-Substitution-Based Satellite Image Fusion by Using Partial Replacement [J]. IEEE Transactions on Geoscience and Remote Sensing, 2011, 49(1): 295-309.

[11] CHAVEZ P S, SIDES S C, ANDERSON J A J P E, SENSING R. Comparison of three different methods to merge multiresolution and multispectral data: Landsat TM and SPOT panchromatic [J]. Photogrammetric Engineering & Remote Sensing, 1991, 57(3): 265-303.

[12] LIU, J. G J I J O R S. Smoothing Filter-based Intensity Modulation: A spectral preserve image fusion technique for improving spatial details [J]. International Journal of Remote Sensing, 2000, 21(18): 3461-72.

[13] King R L, Wang J. A wavelet based algorithm for pan sharpening Landsat 7 imagery [J]. IEEE, 2001, 2:849-851. DOI:10.1109/IGARSS.2001.976657.

[14] AIAZZI B, ALPARONE L, BARONTI S, et al. MTF-tailored Multiscale Fusion of High-resolution MS and Pan Imagery [J]. Photogrammetric Engineering & Remote Sensing, 2006, 72(5): 591-6.

[15] VIVONE G, RESTAINO R, MURA M D, et al. Contrast and Error-Based Fusion Schemes for Multispectral Image Pansharpening [J]. IEEE Geoscience and Remote Sensing Letters, 2014, (5).